NCPMF-60 induces G2/M cell cycle arrest and apoptosis in human hepatocellular carcinoma HepG2 cells

Qin-Sheng Dai[a], Wei Liu[c], Xiao-Bing Wang[b], Na Lu[a], Dan-Dan Gong[a], Ling-Yi Kong[b] and Qing-Long Guo[a]

We recently established that NCPMF-60, a newly synthesized flavonoid, is an active cytotoxic component. The molecular mechanisms by which NCPMF-60 exerts its cytotoxic activity are currently unknown. In this study, we show that NCPMF-60 induces G2/M phase arrest and apoptosis in human hepatocellular carcinoma HepG2 cells. After treatment of HepG2 cells with NCPMF-60, cell cycle-related proteins, such as cyclin B1, cyclin H, CDK7, and p-CDK1 (Thr161), were downregulated, whereas $p21^{WAF1/Cip1}$ and p-CDK1 (Thr14/Tyr15) were upregulated. The activity of CDK1/cyclinB complex was also inhibited by NCPMF-60. In addition, we observed poly(ADP-ribose) polymerase cleavage and activation of caspase 3 and caspase 9. The expression ratio of Bax/Bcl-2 was increased in the treated cells, in which Bax was also upregulated. We also found that the expression of p53 and its phosphorylation at Ser15 accumulated after the treatment of NCPMF-60. Moreover, upregulation of $p21^{WAF1/Cip1}$, p53-upregulated modifier of apoptosis, and Bax, three p53-target gene products, and the downregulation of Bcl-2 and MDM2, were observed in NCPMF-60-treated cells. However, p53 is not the only regulator in the stimulation of NCPMF-60 on p21 transcriptional level and posttranscriptional level. These results suggested that NCPMF-60 indeed activated the p53 pathway, which may contribute to its induction of cell cycle arrest and apoptosis in HepG2 cells. Collectively, our findings show that cell cycle arrest and apoptosis induced by NCPMF-60 was associated with the activation of p53 pathway and the inhibition of CDK-activating kinase activity in HepG2 cells. *Anti-Cancer Drugs* **22:46–57 © 2011 Wolters Kluwer Health | Lippincott Williams & Wilkins.**

Anti-Cancer Drugs 2011, **22**:46–57

Keywords: apoptosis, cell cycle arrest, NCPMF-60, p21, p53

[a]Jiangsu Key Laboratory of Carcinogenesis and Intervention, [b]Department of Natural Medicinal Chemistry, China Pharmaceutical University and [c]Department of Pharmacology, Nanjing Medical University, Nanjing, People's Republic of China

Correspondence to Dr Qing-Long Guo, Jiangsu Key Laboratory of Carcinogenesis and Intervention, China Pharmaceutical University, 24 Tongjiaxiang, Nanjing, Jiangsu 210009, People's Republic of China
Tel/fax: +86 25 83271055; e-mail: anticancer_drug@yahoo.com.cn

Qin-Sheng Dai and Wei Liu have contributed equally

Received 13 April 2010 **Revised form accepted** 8 September 2010

Introduction

Hepatocellular carcinoma (HCC) is the fifth ranking cancer in the world, with more than 80% of cases occurring in Asia. It is also a disease that has increased in incidence in the western world over the past 20 years [1]. Among the current effective treatments for HCC, surgical resection and liver transplantation are the main curative treatments. However, only approximately 20% patients may benefit from these surgical therapies. Most other patients either present late with advanced tumor or have severe underlying cirrhosis, can only be palliated by chemotherapy or best supportive treatment alone [2]. HCC is highly refractory to cytotoxic chemotherapy because of its tumor biology, pharmacokinetic properties, and both intrinsic and acquired drug resistance. Finding new targeted agents or newer combination chemotherapy are still crucial to the treatment of HCC.

The eukaryotic cell cycle is a fundamental evolutionarily conserved process that regulates cell division, which is strictly regulated by a class of cyclins and cyclin-dependent kinases (CDKs) [3]. Cyclins are positive regulatory subunits for CDKs. The complex formation of cyclins with CDKs results in an active agent that phosphorylates substrates involved in cell cycle progression [4]. In normal cell cycles, CDK4 and CDK6 pair with D-type cyclins during G1, CDK2 pairs with E-type and A-type cyclins during S and G2, and CDK1 pairs with A-type and B-type cyclins during G2 and M [5–7]. However, the mitosis-promoting factor, which comprises a complex of CDK1 and cyclin B, is thought to be the key controller of the progression from G2 to mitosis [8–11]. During G2/M transition, CDK1 (cdc2) activation requires association with cyclin partners and phosphorylation by CDK-activating kinase (CAK). CDK7 together with cyclin H and the assembly factor MAT1 forms CAK, responsible for the activation of CDK1, CDK2, CDK4, and CDK6 [12]. Binding to cyclin B and phosphorylation at Thr161 by CAK is required for the activation of CDK1, whereas the CDK1/cyclin B complex is kept inactive by phosphorylation on Thr14 or Tyr15 of CDK1 by kinase Wee1 and Myt1 [13]. The CDC25C phosphatase removes the phosphates of Thr14 and Tyr15 in CDK1, resulting in the activation of the cyclin B/CDK1 complex [5] (Fig. 6).

P53 is a major orchestrator of the cellular response to a broad array of stress types by regulating apoptosis, cell cycle arrest, senescence, DNA repair, and genetic stability. Its functions as a transcription factor have been

0959-4973 © 2010 Wolters Kluwer Health | Lippincott Williams & Wilkins DOI: 10.1097/CAD.0b013e3283405801

well studied for a long time [14]. p53 participates directly in the intrinsic apoptosis pathway by interacting with the multinomial members of the Bcl-2 family to induce mitochondrial outer membrane permeabilization [15]. Aside from its apoptotic function, p53 is also a key regulator in both G1 and G2 growth arrest. The mechanism by which p53 regulates the G2/M transition involves regulation of CDK1, which is essential for entry into mitosis [13]. In addition to modulation of cyclin B1/CDK1 levels and activity by transactivation of p21, p53 also exerts G2 checkpoint responses through transcriptional upregulation of additional downstream target genes, including 14-3-3-σ and GADD45 [16].

NCPMF-60 is a newly synthesized flavonoid (Fig. 1a). In our early experiments of screening efficacious antitumor drugs, NCPMF-60 exerted a strong proliferative inhibitory effect against some certain cancer cells, which makes it a potential antitumor agent for further study. In this study, we assessed the inhibitory effects and molecular mechanisms of NCPMF-60 using human HCC HepG2 cells. The results showed that NCPMF-60 inhibited the growth of HepG2 cells in both time-dependent and concentration-dependent manners and induced G2/M phase cell cycle arrest and apoptosis. We assayed the levels of cell cycle control-related and apoptosis-related molecules, which are strongly associated with the programmed cell death signal transduction pathway and found that p53 played an important role in the anticancer effects of NCPMF-60. All the studies provided a mechanistic framework for further exploring of NCPMF-60 as a promising anticancer agent for human tumors.

Materials and methods

Reagents

NCPMF-60 was obtained from Dr Lingyi Kong (China Pharmaceutical University, China). Samples containing 98% or higher NCPMF-60 were used in all experiments unless otherwise indicated. NCPMF-60 was dissolved in dimethyl sulfoxide (DMSO) with a concentration of 10 mmol/l and stored at −20°C. The concentrations used in this study were 10, 15, and 20 μmol/l. The working solution was freshly prepared in the basal medium with

Fig. 1

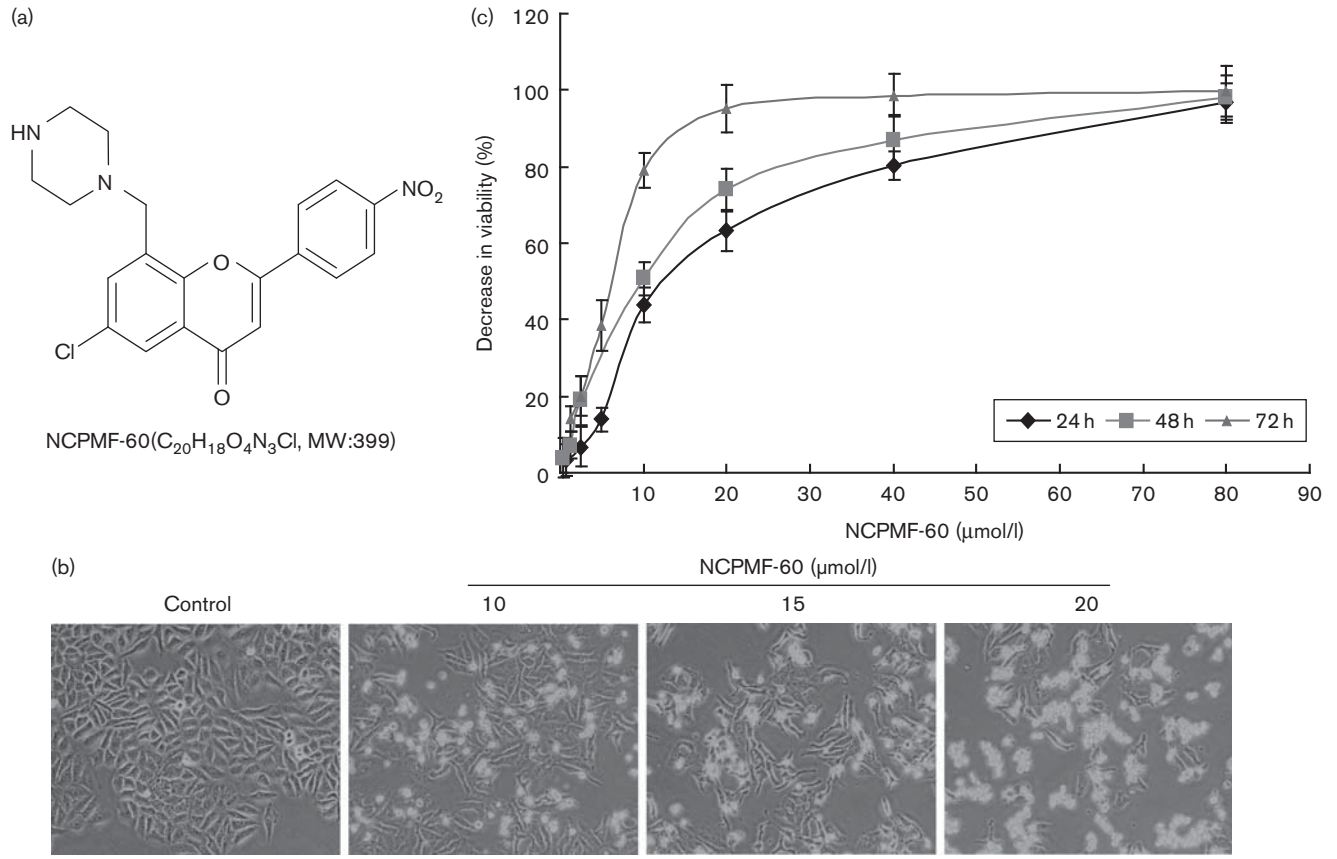

NCPMF-60 inhibits the viability of HepG2 cells. (a) Molecular structure of NCPMF-60 ($C_{20}H_{18}O_4N_3Cl$, MW: 399). (b) HepG2 cells were treated with indicated concentrations of NCPMF-60 for 24 h and then observed under an inverted light microscope. (c) The 3-(4,5-dimethylthiazol-2-yl)-2,5-diphenyltetrazolium bromide assay was used to detect cell viability after treatment of different concentrations of NCPMF-60 for 12, 24, and 48 h, respectively. The data shown are the mean from three parallel experiments (mean ± standard error).

a final DMSO concentration of 0.1%. The controls were treated with the same amount of DMSO as used in the corresponding experiments.

Antibodies of Bax, Bcl-2, caspase 3, caspase 8, caspase 9, MDM2, CDK2, CDK1, p-CDK1 (Thr14/Tyr15), p-CDK1 (Thr161), p-p53 (Ser15), p-p53 (Ser20), cyclin A, cyclin B1, CDK7, and cyclin H were from Santa Cruz (Santa Cruz, California, USA). Antibody of $p21^{WAF1/Cip1}$ was from Upstate Biotechnology (Lake Placid, New York, USA). Antibody of p53 was from EMD Chemicals (Gibbstown, New Jersey, USA). Antibodies of poly(ADP) ribose polymerase (PARP) and p53-upregulated modifier of apoptosis (PUMA) were from Cell Signal (Danvers, Massachusetts, USA). Antibody of β-actin was from Boster (Wuhan, China). IRDyeTM 800 conjugated antimouse and antirabbit second antibodies were obtained from Rockland Inc., (Philadelphia, Pennsylvania). Propidium iodide (PI), ribonuclease, and 3-(4,5-dimethylthiazol-2-yl)-2,5-diphenyltetrazolium bromide (MTT) were purchased from Sigma-Aldrich (St. Louis, Missouri, USA). All the other chemicals were of the highest pure grade.

Cell lines

Human HCC HepG2 cells harboring wild-type p53 were obtained from the Cell Bank of Shanghai, Institute of Biochemistry and Cell Biology, Chinese Academy of Sciences. Cells were cultured in RPMI 1640 (GIBCO, Invitrogen Corporation, New York, USA) supplemented with 10% fetal bovine serum (Sijiqing, Zhejiang, China), 100 U/ml benzyl penicillin, and 100 U/ml streptomycin in a humidified environment with 5% CO_2 at 37°C.

Colorimetric MTT assay

After NCPMF-60 exposure for 24, 48, or 72 h, 20 μl of 5 mg/ml MTT were added to cells, and the cells were incubated at 37°C for another 4 h. The culture medium was then discarded and 0.1 ml DMSO was used to dissolve the precipitate. The absorbance was measured at 570 nm using an Automated Microplated Reader ELx800 (BioTek, BioTek Instruments Inc., Winooski, Vermont, USA). The inhibition ratio (%) was calculated using the following equation: inhibitory ratio (%) = (1 – average absorbance of treated group/average absorbance of control group) × 100%. IC50 was taken as the concentration that caused 50% inhibition of cell viabilities and calculated by the Logit method.

Cell morphological assessment

Cells were seeded in six-well tissue culture plates and treated with the indicated concentrations of NCPMF-60. At the end of each incubation, cell morphology was monitored using an inverted light microscope. For fluorescence analysis, cells were fixed with 4% paraformaldehyde for 20 min, washed with PBS, and then incubated with 4′,6-diamidino-2-phenylindole (1 μg/ml) for 10 min. After washing with PBS, the cells were observed using a fluorescence microscope (Olympus, Japan) with a peak excitation wavelength of 340 nm.

Cell cycle analysis

Cells treated for different time periods were trypsinized, washed with PBS, and fixed in 100% ethanol for 1 h at –20°C. The cells were then washed with PBS and stained with PI (Sigma) containing 0.05% ribonuclease. For cell cycle analysis, DNA content was determined using a FACScan laser flow cytometer (FACSCalibur, Becton Dickinson, USA). Data were analyzed using MODFIT and CELLQUEST software (Verity Software House, Topsham, Maine, USA).

AnnexinV/propidium iodide staining

Apoptosis-mediated cell death of HepG2 cells was examined using a fluorescein isothiocyanate-labeled AnnexinV/PI Apoptosis Detection Kit (BioVision, Mountain View, California, USA) according to the manufacturer's instructions. Briefly, 1×10^6 cells were harvested and washed with PBS. The cells were resuspended in 500 μl binding buffer. Next, 5 μl annexin-V–fluorescein isothiocyanate and 1 μl PI was added. Flow cytometric analysis was done immediately after supravital staining. Data acquisition and analysis were carried out in a Becton Dickinson FACSCalibur flow cytometer using CELLQUEST software. The cells in early stages of apoptosis were annexin V positive and PI negative, whereas the cells in the late stages of apoptosis were both annexin V and PI positive.

Western blotting assay

Cells were collected and lysed in a lysis buffer (100 mmol/l Tris–Cl, pH 6.8, 4% (m/v) SDS, 20% (v/v) glycerol, 200 mmol/l β-mercaptoethanol, 1 mmol/l phenylmethylsulfonyl fluoride, and 1 g/ml aprotinin). Lysates were then centrifuged at 12 000*g* for 15 min at 4°C. The supernatant was collected, and total protein concentrations were determined using the BCA assay by Varioskan spectrofluorometer and spectrophotometer (Thermo, Waltham, Massachusetts, USA). Samples were separated on 10–15% SDS–polyacrylamide gel electrophoresis and transferred to polyvinylidene fluoride membranes (Millipore, Billerica, Massachusetts, USA). Immune complexes were formed by incubating proteins with primary antibodies overnight at 4°C followed by incubation with IRDye800 conjugated secondary antibodies for 1 h at 37°C. Immunoreactive protein bands were detected with an Odyssey Scanning System (LI-COR Inc., Superior St. Lincoln, Nebraska, USA).

CDK1/cyclin B kinase activity assay

CDK1/cyclin B kinase activity was measured using a CDK1/cyclin B kinase activity assay kit according to the manufacturer's instruction (Genmed Scientifics Inc., USA, Arlington, Massachusetts, USA). The assay was used to detect the change of absorption peak, which represents the CDK1/cylin B kinase activity. Briefly,

500 μl cell lysates were obtained from 1×10^6 cells in lysis buffer, incubated for 30 min on ice, and then centrifuged at 16000 *g* for 5 min at 4°C. After the concentration of total proteins was measured, supernatants containing 50 μg total protein were incubated with 10 μl substrate, 10 μl reacting solution, 10 μl enzymatic solution, and 65 μl buffer solution at 30°C for 3 min. Absorbance at 340 nm was determined. The activity of the CDK1/cyclin B was calculated as following:

$$\text{Kinease activity}\,(\mu\text{mol/l NADH/min/mg}) = \frac{(\text{OD}_{\text{sample}} - \text{OD}_{\text{blank}}) \times \text{dilute multiple}_{\text{sample}} \times 0.1}{0.005 \times 6.22 \times 0.6 \times 5}$$

Small-interference RNA transfection

Small-interfering RNA of p53 and irrelevant control siRNA were purchased from Santa Cruz. For transfection, HepG2 cells were seeded in six-well plates at 50–70% confluency, and either p53 siRNA duplexes (30 pmol/μl) or irrelevant control siRNA were introduced into the cells using Lipofectamine 2000 (Invitrogen, California, USA) according to the manufacturer's recommendations. After that, the cells were exposed to NCPMF-60 or the vehicle and harvested for further experiments.

Reverse transcription-PCR assay

Total cellular RNA was extracted from NCPMF-60-treated HepG2 cells using the TriPure solution following the manufacturer's instructions. The purity of the RNA extracted was determined by the ratio of A260/A280 using a BioPhotometer (Eppendorf, Germany). Reverse transcription-polymerase chain reaction was performed by Primescript reverse transcriptase (Takara, Takara Bio Inc., Otsu, Shiga, Japan) following the manufacturer's instructions. The amplified PCR products were separated by electrophoresis on a 2% agarose gel containing ethidium bromide and quantified by relative intensities of the bands compared with those of β-actin using Gel Base/Gel Blot/Gel Excel/Gel Sequence analysis software (UVP, UK). A value of 100% was given to the relative intensity of untreated cells (control). The sequences of the PCR primers and the expected size of amplicons were as follows: $p21^{WAF1/Cip1}$ (316 bp) 5′-CCC GTG AGC GAT GGA AC T-3′ (sense) and 5′-CGA GGC ACA AGG GTA CAA GA-3′ (antisense); p53 (497 bp) 5′-TGC TCA GAT AGC GATG GT C-3′ (sense) and 5′-TTT ATG GCG GGA GGT AGA-3′ (antisense); glyceraldehyde 3-phosphate dehydrogenase (372 bp) 5′-CAC CAT CTT CCA GGA GCG AG-3′ (sense), and 5′-TCA CGC CAC AGT TTC CCG GA-3′ (antisense).

Statistics

All results are presented as means ± standard error of mean from triplicate experiments carried out in a parallel manner unless otherwise indicated. Statistical analyses were done using one-way analysis of variance, followed by the Bonferroni posttest for multiple group comparisons. All comparisons are made relative to untreated controls and significant differences are indicated as $^*P < 0.05$ and $^{**}P < 0.01$.

Results

NCPMF-60 inhibits the viability of HepG2 cells

As shown in Fig. 1b, untreated HepG2 cells grew well with clear skeletons, whereas cells treated with NCPMF-60 were distorted and some became round. The sloughed cells increased with increasing drug concentrations. An MTT assay showed that NCPMF-60 significantly inhibited the viability of HepG2 cells (Fig. 1c). The cells were incubated in the absence or presence of different concentrations of NCPMF-60 for specified time periods (24, 48, and 72 h), and IC_{50} values were 12.91 ± 0.26, 10.35 ± 0.73, and 4.52 ± 0.32 μmol/l for 24, 48, and 72 h, respectively. The MTT assay showed that NCPMF-60 decreased the viability of HepG2 cells in a concentration-dependent and time-dependent manner.

NCPMF-60 induces the G2/M phase cell cycle arrest and apoptosis in HepG2 cells

To investigate whether NCPMF-60 affects the cell cycle of HepG2 cells, the cell cycle distribution of synchronized cells treated with or without NCPMF-60 were analyzed by measuring the DNA content with PI after exposure to NCPMF-60 for 24 h. As shown in Fig. 2a, compared with control group, cells showed a statistically significant accumulation in the G2/M fraction accompanied by a decrease in the G0/G1 and S fraction. In contrast to a vehicle control, the percentage of cells in the G2/M fraction increased 3.7-fold when treated with 20 μmol/l NCPMF-60. In addition, as shown in Fig. 2b, the G2/M phase cell cycle arrest was evident as early as 6 h after treatment with 20 μmol/l NCPMF-60, and persisted for the duration of the experiment. In addition, NCPMF-60 seems to induce an increase in the number of cells with a sub-G1 DNA content at 20 μmol/l, indicating an increase in the number of apoptotic cells, which is consistent with the result of the apoptotic assay below. These results showed that NCPMF-60 exerted its effect of G2/M phase cell cycle arrest induction in HepG2 cells, which contributed to the effects of NCPMF-60 on decreasing viability against HepG2 cells.

Apoptosis is another hallmark of carcinogenesis aside from cell cycle arrest. To identify the apoptotic effect induced by NCPMF-60, we examined its induction of biochemical events in HepG2 cells. After treating with NCPMF-60 for 24 h, cells presented morphological features of early apoptosis, such as bright, nuclear condensation, and apoptotic bodies. These features seemed to be more frequent with increasing concentrations of NCPMF-60 (Fig. 2c). Annexin-V/PI staining assay was used for further analysis of NCPMF-60-induced

Fig. 2

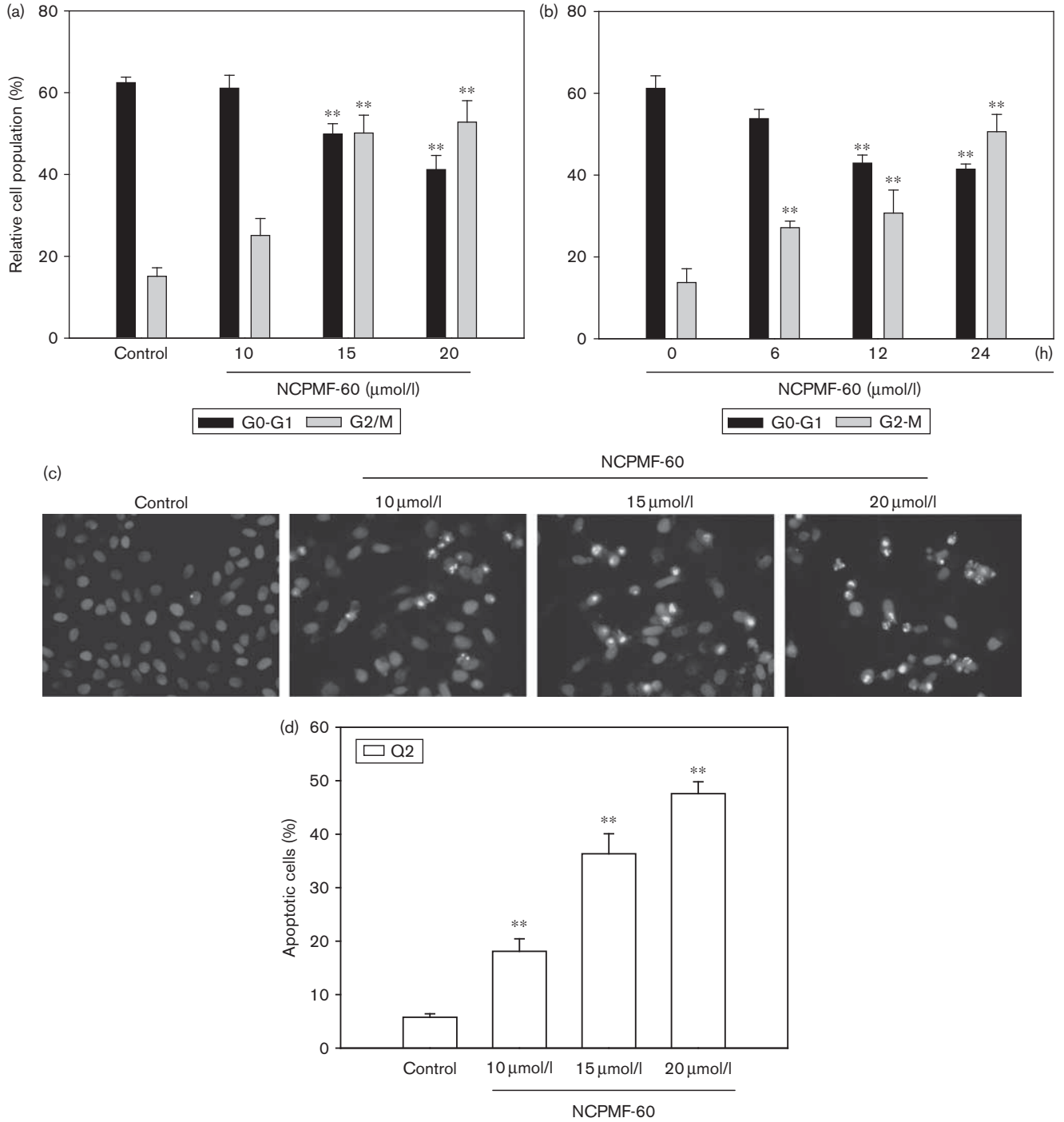

NCPMF-60 induces G2/M cell cycle arrest and apoptosis in HepG2 cells. (a) Histogram of cell cycle distribution after treatment with 10, 15, and 20 μmol/l of NCPMF-60 for 24 h. Each histogram represents three parallel experiments, and each bar represents the mean ± standard error (SEM) [one-way analysis of variance (ANOVA)]. $^{**}P<0.01$ indicates a significant difference between control and NCPMF-60-treated cells (15, 20 μmol/l). (b) Histogram of cell cycle distribution after treatment with or without 20 μmol/l NCPMF-60 for 0, 6, 12, and 24 h, respectively. Cell cycle distribution was monitored by flow cytometry using propidium iodide staining assay. Each histogram represents three parallel experiments, and each bar represents the mean ± SEM (one-way ANOVA). $^{**}P<0.01$ indicates a significant difference between 0 h and 20 μmol/l NCPMF-60-treated cells at 6, 12, and 24 h. (c) 4′,6-diamidino-2-phenylindole staining of HepG2 cells after treatment with NCPMF-60 (10, 15, and 20 μmol/l) for 24 h. (d) Histogram of apoptosis cell distribution with or without NCPMF-60 treatment for 24 h. Each histogram represents three parallel experiments, and each bar represents the mean ± SEM (one-way ANOVA). $^{**}P<0.01$ indicates a significant difference between control and NCPMF-60-treated cells (10, 15, 20 μmol/l).

apoptosis. The early stage of apoptosis is readily detectable by annexin V whereas the later stage of apoptosis is detected by PI that can move across the cell membrane to bind to cellular DNA. As shown in Fig. 2d, after treating with 10, 15, and 20 μmol/l NCPMF-60 for 24 h, the early-to-mid-apoptotic cells represented 18.1%, 36.3%, and 47.6% of the total cells, respectively, compared with the control group with only 5.8% apoptotic cells. The effects were statistically significant at 10, 15, 20 μmol/l of NCPMF-60 treatment compared with control group (one-way analysis of variance). Meanwhile, the late apoptotic and necrotic cells have no changes (data not shown). Collectively, these results suggest that induction of G2/M cell cycle arrest and apoptosis by NCPMF-60 involves its antitumor activity.

Effects of NCPMF-60 treatment on the expression of cell cycle regulatory and apoptotic-related proteins

To gain insight into the mechanism of G2/M phase cell cycle arrest induced by NCPMF-60, we examined the expression of cyclins, CDKs, CDKI, and CAK, which are tightly related with G2/M cell cycle progression, using the western blot assay. As shown in Fig. 3a, the expression of cyclin B1, CDK7, and cyclin H was decreased to varying degrees after NCPMF-60 treatment for 24 h. However, no changes were observed in the expression levels of cyclin A, CDK1, and CDK2. Cell exposure to NCPMF-60 also resulted in an increase in the protein level of $p21^{WAF1/Cip1}$, p-CDK1 (Thr14/Tyr15), and a decrease in p-CDK1 (Thr161). These results show that NCPMF-60-induced cell cycle arrest is due in part to the

Fig. 3

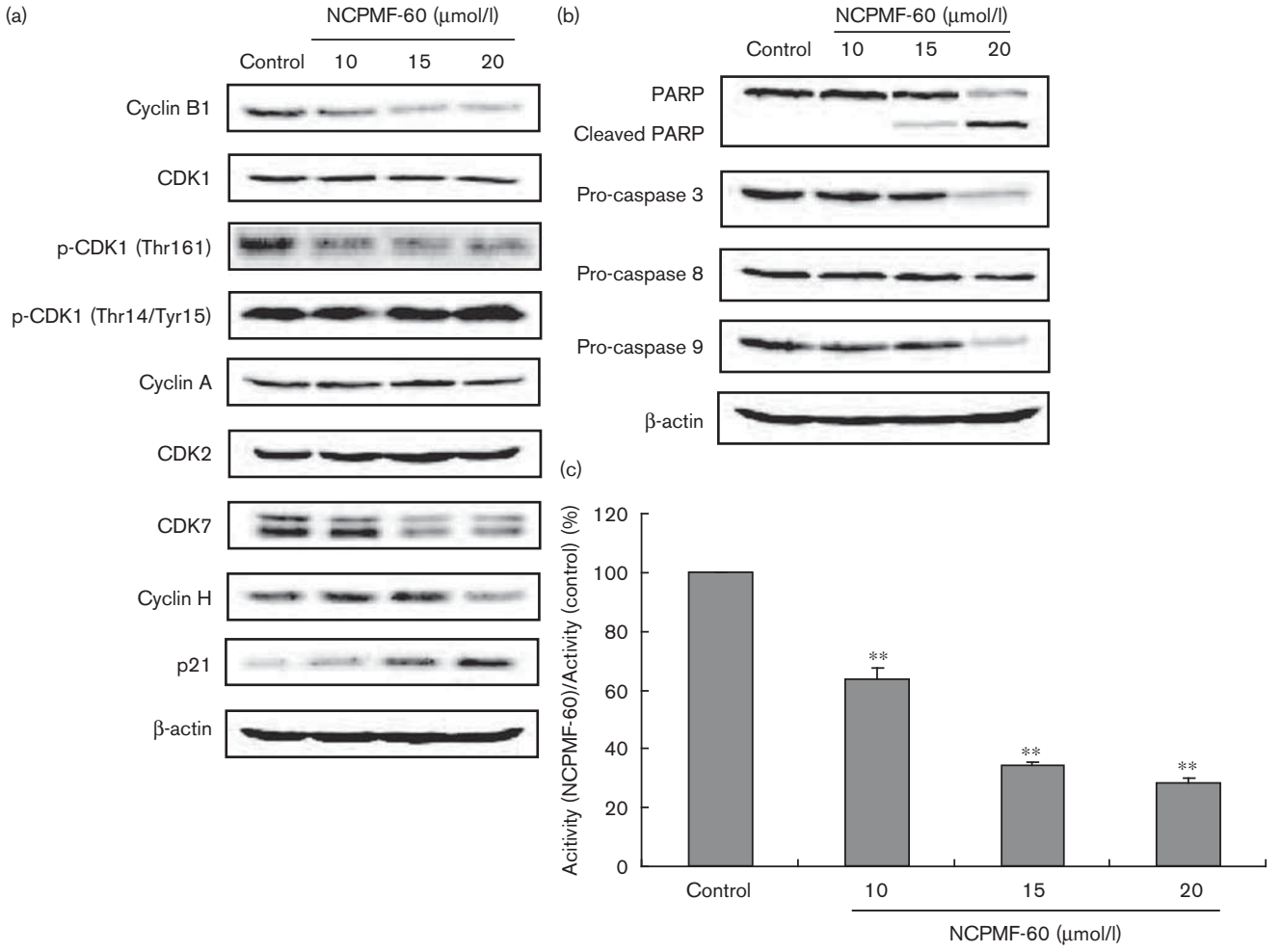

Expression of cell cycle regulatory proteins and apoptosis-related proteins in HepG2 cells treated with NCPMF-60 and the effect of NCPMF-60 on CDK1/cylin B kinase activity. Cells were treated with different concentrations of NCPMF-60 for 24 h. (a) The levels of cyclin A, cyclin B1, CDK1, CDK2, p-CDK1 (Thr161), p-CDK1(Thr14/Tyr15), cyclin H, CDK7, and p21 were detected by western blot assay. (b) The levels of apoptosis-related proteins including poly-ADP-ribose polymerase, pro-caspase 3, pro-caspase 9, and pro-caspase 8 were assessed by western blot assay. (c) The CDK1/cylin B kinase activity was detected using the method mentioned above, each histogram represents three parallel experiments, and each bar represents the mean ± SEM (one-way ANOVA).

changes in the cyclin B1, p-CDK1 (Thr14/Tyr15), p-CDK1 (Thr161), $p21^{WAF1/Cip1}$, cyclin H, and CDK7 protein levels.

PARP is the substrate for effector caspases during apoptosis, which is involved in DNA repair, genome surveillance, and maintenance of genomic integrity in response to environmental stress [17]. The cleavage of PARP is the hallmark of apoptosis. Caspase-mediated PARP cleavage showed that NCPMF-60-induced apoptosis was concentration-dependent (Fig. 3b). We further examined the involvement of caspases in NCPMF-60-mediated apoptosis. Compared with the control group, caspase 3 and caspase 9 were both activated after the treatment for 24 h, whereas the expression of caspase 8 remained unchanged. The effect seems obvious at 20 μmol/l, with a sharp change over a narrow concentration range (between 15 and 20 μmol/l). Moreover, the apoptotic protein Bax increased whereas antiapoptotic protein Bcl-2 decreased (Fig. 4a). Thus, the ratio of Bax/Bcl-2, which is crucial for the activation of the mitochondrial apoptotic pathway, increased in cells treated with NCPMF-60. These results indicated that the intrinsic apoptotic pathway, not the extrinsic apoptosis way, is involved in NCPMF-60-induced apoptosis in HepG2 cells.

Fig. 4

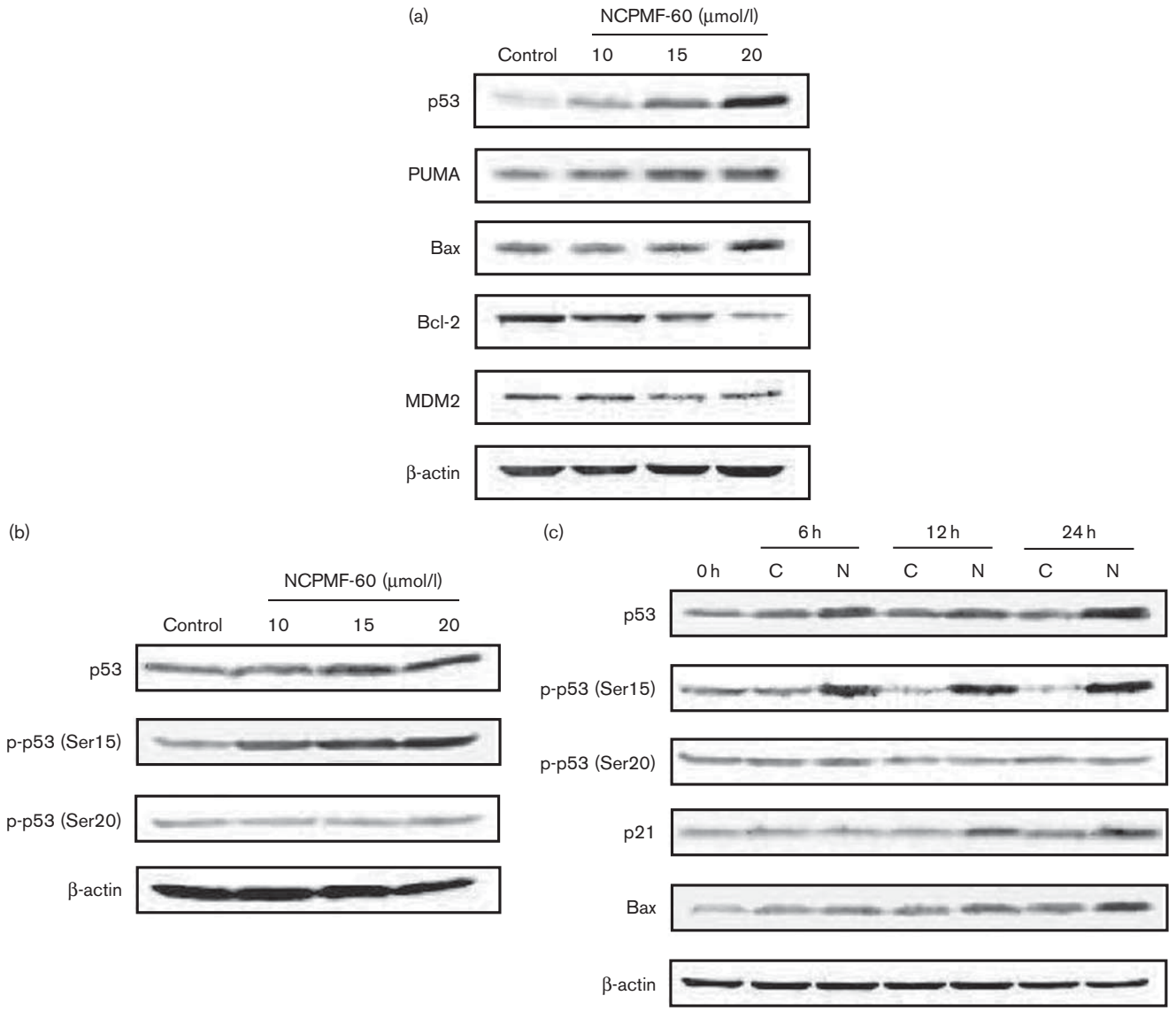

Effects of NCPMF-60 on the activation of p53 and p53 pathway. (a) The levels of p53 pathway-related proteins including Bax, Bcl-2, PUMA, MDM2, and p53 were detected by western blot assay after NCPMF-60 treatment for 24 h. (b) The levels of p53, p-p53 (Ser15), and p-p53 (Ser20) were detected by western blot assay after NCPMF-60 treatment for 24 h. (c) The levels of p53, p-p53 (Ser15), and p-p53 (Ser20) were detected by western blot assay after 20 μmol/l NCPMF-60 treatment for 0, 6, 12, and 24 h. C, control and N, NCPMF-60.

NCPMF-60 inhibits CDK1/cyclin B kinase activity in HepG2 cells

The progression from G2 to mitosis is mainly regulated by the activation of CDK1/cyclin B complex, whose activity may play a role in protein synthesis control [18]. The reduced expression of CDK1/cyclin B is mediated in part by p53-dependent repression of the cyclin B1 and CDK1 promoters and several transcriptional downstream targets [16]. Western blot showed that NCPMF-60 decreased the expression of cyclin B1 and p-CDK1 (Thr161) protein increased the expression of p-CDK1 (Thr14/Tyr15) (Fig. 3a). Therefore, we further explored the effect of NCPMF-60 on the activity of CDK1/cyclin B complex. The values of CDK1/cyclin B activity were calculated using the formula mentioned in the method above. Comparisons of the activity among the NCPMF-60-treated groups and the control group have been made. As shown in Fig. 2c, the ratio of activity NCPMF-60-treated group/activity$_{(control)}$ are 63.54%, 34.08%, and 28.16% for 10, 15, and 20 μmol/l, respectively. These data indicated that the activity of CDK1/cyclin B was significantly inhibited by NCPMF-60 treatment (at 10, 15, and 20 μmol/l, respectively), compared with the control group.

Role of p53 pathway in NCPMF-60-mediated cell cycle arrest and apoptotic effects in HepG2 cells

Tumor suppressor p53 has a central role in eliciting the cellular responses to various cellular stresses [19]. The stabilization and activation of p53 result in two major outcomes: cell cycle arrest or apoptotic cell death [20]. Thus, we suppose that the p53 pathway may be involved in NCPMF-60-induced G2/M phase arrest and apoptosis. We detected the expression of p53 pathway-related proteins. As shown in Fig. 4a, the expression of p53 accumulated in a concentration-dependent manner after the treatment of NCPMF-60 for 24 h. Moreover, upregulation of p21, PUMA, and Bax, three p53-target gene products, and the downregulation of Bcl-2 and MDM2, were observed in NCPMF-60-treated cells. These results suggested that NCPMF-60 indeed activated the p53 pathway, which may contribute to its induction of cell cycle arrest and apoptosis in HepG2 cells.

Activation of p53 is associated with protein phosphorylation on Ser 15 through the atxia–telangiectasia mutated kinase (ATM), Rad3-related kinase (ATR), and DNA-dependent protein kinase signaling pathway [21]. Chk2 and Chk1 can phosphorylate p53 at Ser20, enhancing its tetramerization, stability, and activity [22]. As shown in Fig. 4b, NCPMF-60 treatment resulted in an accumulation of p53 and phosphorylation at Ser15, whereas no marked changes were observed in the expression of p-p53 (Ser 20). Accordant results were observed after treating with 20 μM NCPMF-60 for 0, 6, 12, and 24 h (Fig. 4c). Moreover, the upregulation of p21 expression was observed obviously as early as 12 h after NCPMF-60 treatment, whereas the increased expression of Bax seemed notable at 24 h after treatment. These data indicated that p53 is activated before the observed cell cycle response occurs.

The linkage of p53 activation to CDK1 inhibition is mainly mediated by p21, which is known to directly inhibit the CDK1/cyclin B complex [23]. To further explore the role of p53 pathway in NCPMF-induced cell cycle arrest and apoptosis in HepG2 cells, the expression of p53 was decreased by siRNA. Compared with irrelevant control siRNA group, p53 siRNA-transfected cells displayed less increase in expression after NCPMF-60 treatment. The upregulation of PUMA and downregulation of MDM2 induced by NCPMF-60 were markedly inhibited after p53 silencing. Interestingly, the expression of $p21^{WAF1/Cip1}$ remained increased in NCPMF-60 treatment group after p53 silencing. However, the extent of $p21^{WAF1/Cip1}$ upregulation induced by NCPMF-60 in p53 siRNA group was slightly attenuated than that of irrelevant control siRNA group (Fig. 5a). Similar results were obtained in reverse transcription-polymerase chain reaction assay. As shown in Fig. 5b, the mRNA level of p21 was reduced appreciably after p53 silencing, whereas it could still be induced by NCPMF-60. These data showed that knockdown of p53 significantly disrupt the ability of NCPMF-60 on induction of PUMA and reduction of MDM2, which are two p53 target genes. Knockdown of p53 prevents the stimulation in p21 transcription level and posttranscription level to some extent after NCPMF-60 treatment, but the stimulation on p21 expression of NCPMF-60 may also be regulated by other regulators except for p53.

Discussion

Recently, the process of searching for new cancer drugs has moved from a strategy identifying drugs that kill tumor cells toward a more mechanistic strategy acting on molecular targets that undergo cell transformation [24]. The rationale for targeting the cell cycle and, in particular, the CDKs in anticancer therapy has been based on the frequency of their perturbations in human malignancy and the observation that cell cycle arrest by CDK inhibition could induce apoptosis. This rationale led to the development of CDKIs as novel antitumor agents [25]. Flavonoids are ubiquitous plant metabolites with a wide range of biological activities. Some flavones can act as antineoplastic agents and are known to perturb the cell cycle progression and modulate CDKs activity in different types of human cancers [26]. For example, flavopiridol, a semisynthetic flavone analog of a natural product extracted from *Dysoxylum benectariferum*, is now best classified as a CDKI because of its considerable affinity for CDKs to induce cell cycle arrest in a number of cell lines, and its several other anticancer activites [24–26]. In our early studies, NCPMF-60, a newly synthesized flavonoid, exerts its growth-inhibitory effects in cancer cells. On the basis of the similarity of the structure and the anticancer activities of flavonoids, we supposed that NCPMF-60 could be a promising anticancer agent. In this

Fig. 5

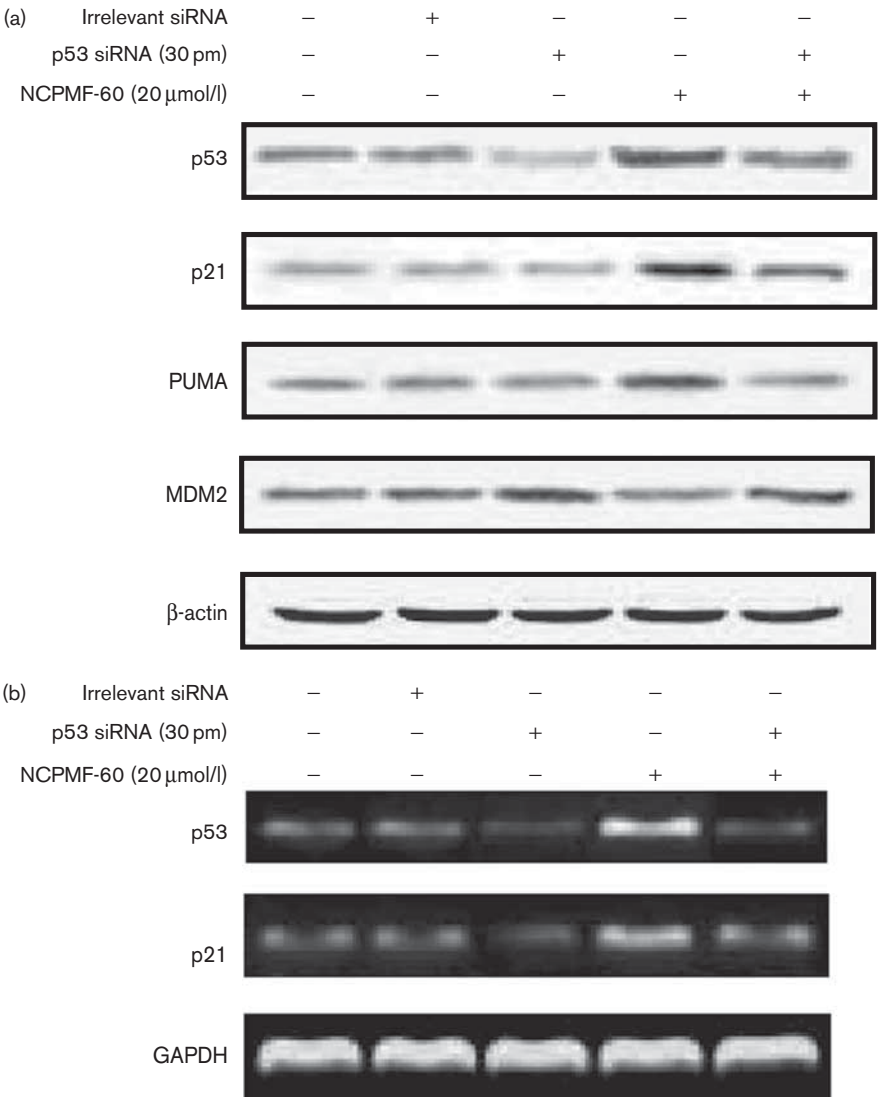

Role of the p53 pathway in the NCPMF-60 responsive cell cycle/apoptotic response. (a) Expression of p53, p21, p53-upregulated modifier of apoptosis (PUMA), and MDM2 were detected by western blot assay in p53 siRNA-transfected HepG2 cells. (b) Expression of p53 and p21 in mRNA levels were detected by western blot assay in p53 siRNA-transfected HepG2 cells. Cells were treated with or without 20 μmol/l NCPMF-60 for 24 h.

study, we characterized the mechanisms by which NCPMF-60 exerts its inhibitory effects on HepG2 cells by inducing G2/M cell cycle arrest and apoptosis.

Progression through mitosis requires the coordinated regulation of CDK1 kinase activity. Activation of CDK1 is a multistep process comprising binding of CDK1 to cyclin B, relocation of cyclin-kinase complexes to the nucleus, and the regulation of its phosphorylation status. CDK1 activity is triggered both by an activating phosphorylation at Thr161 by CAK and inhibitory phosphorylations at Thr14/Tyr15 by the kinase Wee1 and Myt1 [25]. Cdc25 also dephosphorylates the CDK1/cyclin B complex by removing the inhibitory phosphorylations at Thr14 and Tyr15 on CDK1, which leads to the onset of mitosis [26] (Fig. 6). In our study, we showed that NCPMF-60 induced G2/M cell cycle arrest and repressed the activity of CDK1/cyclin B complex (Fig. 3c). Furthermore, we found that NCPMF-60 decreased the expression of cyclin B and caused a great loss in expression of CDK7 and cyclin H. Besides, NCPMF-60 also resulted in an increase in the protein levels of p-CDK1 (Thr14/Tyr15) and a decrease in p-CDK1 (Thr161). The results indicated that NCPMF-60-mediated G2/M cell cycle arrest correlates with the inhibitory activity of the CDK1/cyclin B1 kinase complex, which is regulated partly by the decrease of cyclin B, the phosphorylation of CDK1 at Thr161 and Thr14/Tyr15, and the activation of CAK (Fig. 3a).

Fig. 6

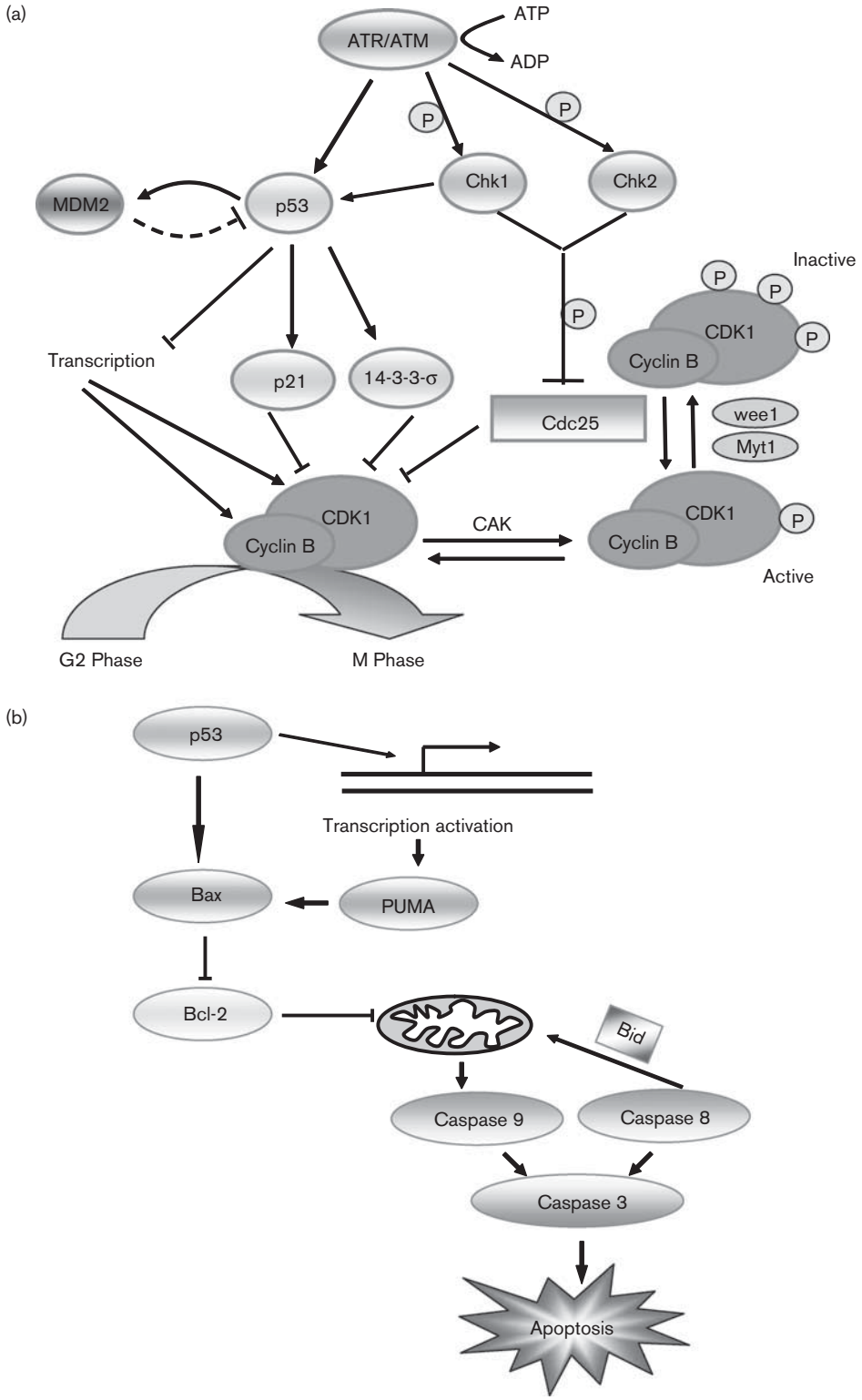

Participation of p53 in regulating G2/M cell cycle arrest and apoptosis. (a) G2 checkpoint response after genotoxic stress. (b) p53-mediated apoptotic signaling.

It has been well established that CDK1 activity is in part determined by its phosphorylation status. The modulation of CDK1 phosphorylation can be divided into two different pathways in response to DNA damage: a p53-independent pathway and a p53-dependent pathway. The major p53-independent mechanism that causes G2 arrest is through the ATM/ATR inactivation of CDK1 by increasing phosphorylation of the residues at Tyr15 and Thr14 [13]. ATM/ATR can phosphorylate and activate the serine kinase Chk1 and Chk2, and the latter ones can phosphorylate Cdc25. Phosphorylated Cdc25 is sequestered in the cytoplasm by 14-3-3 proteins, which prevents activation of cyclin B/CDK1 by Cdc25 and results in G2 arrest [22]. In addition, activated ATM/ATR also participates in the phosphorylation of p53, leading to its stabilization and accumulation in the nucleus [27]. Phosphorylation of p53 at Ser15 points toward by ATM, whereas Chk1 and Chk2 can inactivate Cdc25C by inhibitory phosphorylation of Tyr162 and directly activate p53 by phosphorylation at Ser20. In our study, we showed that NCPMF-60 activated p53 by phosphorylation at Ser15, not at Ser20 (Fig. 4b and c). In addition, NCPMF-60 also stimulated the p53 pathway by upregulating PUMA, bax, p21, and downregulating MDM2 (Fig. 4a). The induction of PUMA and MDM2 by NCPMF-60 are in a p53-dependent manner (Fig. 5a). Further studies will focus on the effects of NCPMF-60 in regulating the upstream kinases of p53.

The other mechanism of p53-dependent G2 arrest involves an initial inhibition of cyclin B1/CDK1 activity by p21 and a subsequent reduction of cyclin B1 and CDK1 protein levels. In this study, we focus our attention on the mechanism of p53-dependent G2 arrest. The results indicated that NCPMF-60 significantly increases the expression of p53 and p21 at both mRNA and protein levels. However, p53 is not the only regulator of p21 on NCPMF-60-induced upregulation of p21 (Fig. 5). This may occur because p21 can be stimulated by many pathways that are independent of p53. Several of the transcriptional inducers of p21, such as nerve growth factor, progesterone, Ca^{2+}, or the transcription factors BETA2 and MYOD1, cooperate with the transcriptional coactivator p300-CREBBP to activate the CDKN1A promoter [28]. In addition to modulation of cyclin B1/CDK1 levels and activity by transactivation of p21, p53 also exerts G2 checkpoint responses through transcriptional upregulation of additional downstream target genes, namely 14-3-3σ, and GADD45 [16]. An additional mechanism by which p53 causes G2 arrest involves regulation of the subcellular localization of CDK1. In addition, p53 can directly reduce the tyrosine phosphorylation of CDK1. p53 also has other targets that do not affect cdc2 but also contribute to G2 arrest [13].

The arrest of cell cycle progression at the G2 phase provides an opportunity for cells to either undergo repair mechanisms or follow the apoptotic pathway. Activation of the caspase cascade in a chain reaction-like manner and subsequent cleavage of its downstream targets are the biochemical hallmark of apoptotic cell death [29]. The activation of caspase 3 plays a crucial role in the initiation of apoptosis. The extrinsic apoptosis pathway involves the activation of caspase 8 by engaging certain members of the tumor necrosis factor family with death receptors on cell surface; the intrinsic apoptosis pathway involves the induction of major outer membrane protein in mitochondria with subsequent formation of the apoptosome (a complex between cytochrome c/Apaf-1/procaspase-9 complex) [29,30]. In addition, extrinsic and intrinsic apoptotic pathways are linked to the actions of Bid. As shown in Fig. 3b, PARP cleavage and the activation of caspase 3 and caspase 9 were observed after NCPMF-60 treatment, whereas no change was observed on the expression of caspase 8. Our results indicated that the intrinsic pathway, not the extrinsic pathway may be involved in NCPMF-60-induced apoptosis. p53-mediated apoptosis can be mediated in both transcription-dependent and transcription-independent pathway (Fig. 6b). As a transcription factor, p53 can induce proapoptotic Bcl-2 members (Bax, PUMA, Noxa, and Bid), and repress the transcription of certain antiapoptotic genes (Bcl-2, Bcl-xL, and survivin). The hallmark of the transcription-independent pathway in p53-mediated apoptosis is the stress-induced accumulation of p53 in cytosol or mitochondria, which leads to the direct activation of Bax and/or Bak [31]. In addition, p53-dependent induction of insulin-like growth factor binding protein 3 induces apoptosis by blocking insulin-like growth factor-1 receptor survival signaling. p53 may mediate mitochondrial signaling by elevation of reactive oxygen species through PIG3 and PIG8 induction [16].

In conclusion, our study has shown that NCPMF-60-induced G2/M cell cycle arrest through the regulation of the phosphorylation of CDK1 and triggers apoptosis in an intrinsic pathway in HepG2 cells. The activation of p53 pathway and the inhibition of CAK activity may contribute to G2/M phase arrest. These results provide an in-vitro proof of concept for NCPMF-60 as a potential agent with antitumor activity in the drug discovery work.

References

1 O'Neil BH, Venook AP. Hepatocellular carcinoma: the role of the North American GI Steering Committee Hepatobiliary Task Force and the advent of effective drug therapy. *Oncologist* 2007; **12**:1425–1432.

2 Yau T, Chan P, Epstein R, Poon RT. Evolution of systemic therapy of advanced hepatocellular carcinoma. *World J Gastroenterol* 2008; **14**:6437–6441.

3 Suryadinata R, Sadowski M, Sarcevic B. Control of cell cycle progression by phosphorylation of cyclin-dependent kinase (CDK) substrates. *Biosci Rep* 2010; **30**:243–255.

4 Yu J, Guo QL, You QD, Zhao L, Gu HY, Yang Y, *et al.* Gambogic acid-induced G2/M phase cell-cycle arrest via disturbing CDK7-mediated phosphorylation of CDC2/p34 in human gastric carcinoma BGC-823 cells. *Carcinogenesis* 2007; **28**:632–638.

5 Choi HJ, Lim do Y, Park JH. Induction of G1 and G2/M cell cycle arrests by the dietary compound 3,3′-diindolylmethane in HT-29 human colon cancer cells. *BMC Gastroenterol* 2009; **9**:39.

6 Chung JH, Bunz F. Cdk2 is required for p53-independent G2/M checkpoint control. *PLoS Genet* 2010; **6**:e1000863.
7 Sanchez I, Dynlacht BD. New insights into cyclins, CDKs, and cell cycle control. *Semin Cell Dev Biol* 2005; **16**:311–321.
8 Yen CY, Chiu CC, Chang FR, Chen JY, Hwang CC, Hseu YC, *et al.* 4beta-Hydroxywithanolide E from *Physalis peruviana* (golden berry) inhibits growth of human lung cancer cells through DNA damage, apoptosis and G2/M arrest. *BMC Cancer* 2010; **10**:46.
9 Stan SD, Zeng Y, Singh SV. Ayurvedic medicine constituent withaferin a causes G2 and M phase cell cycle arrest in human breast cancer cells. *Nutr Cancer* 2008; **60** (**Suppl 1**):51–60.
10 Dvory-Sobol H, Cohen-Noyman E, Kazanov D, Figer A, Birkenfeld S, Madar-Shapiro L, *et al.* Celecoxib leads to G2/M arrest by induction of p21 and down-regulation of cyclin B1 expression in a p53-independent manner. *Eur J Cancer* 2006; **42**:422–426.
11 Doree M, Hunt T. From Cdc2 to Cdk1: when did the cell cycle kinase join its cyclin partner? *J Cell Sci* 2002; **115**:2461–2464.
12 Lolli G, Johnson LN. CAK-cyclin-dependent activating kinase: a key kinase in cell cycle control and a target for drugs? *Cell Cycle* 2005; **4**:572–577.
13 Taylor WR, Stark GR. Regulation of the G2/M transition by p53. *Oncogene* 2001; **20**:1803–1815.
14 Laptenko O, Prives C. Transcriptional regulation by p53: one protein, many possibilities. *Cell Death Differ* 2006; **13**:951–961.
15 Vaseva AV, Moll UM. The mitochondrial p53 pathway. *Biochim Biophys Acta* 2009; **1787**:414–420.
16 Pietenpol JA, Stewart ZA. Cell cycle checkpoint signaling: cell cycle arrest versus apoptosis. *Toxicology* 2002; **181-182**:475–481.
17 Kang J, Lee DK, Lee CH. Cell cycle arrest and cytochrome c-mediated apoptotic induction in human lung cancer A549 cells by MCS-C2, an analogue of sangivamycin. *J Microbiol Biotechnol* 2010; **20**:428–432.
18 Le Breton M, Cormier P, Belle R, Mulner-Lorillon O, Morales J. Translational control during mitosis. *Biochimie* 2005; **87**:805–811.
19 Vazquez A, Bond EE, Levine AJ, Bond GL. The genetics of the p53 pathway, apoptosis and cancer therapy. *Nat Rev Drug Discov* 2008; **7**:979–987.
20 Schuler M, Green DR. Mechanisms of p53-dependent apoptosis. *Biochem Soc Trans* 2001; **29**:684–688.
21 Millau JF, Bastien N, Drouin R. P53 transcriptional activities: a general overview and some thoughts. *Mutat Res* 2009; **681**:118–133.
22 Wang Y, Ji P, Liu J, Broaddus RR, Xue F, Zhang W. Centrosome-associated regulators of the G(2)/M checkpoint as targets for cancer therapy. *Mol Cancer* 2009; **8**:8.
23 Gaul L, Mandl-Weber S, Baumann P, Emmerich B, Schmidmaier R. Bendamustine induces G2 cell cycle arrest and apoptosis in myeloma cells: the role of ATM-Chk2-Cdc25A and ATM-p53-p21-pathways. *J Cancer Res Clin Oncol* 2008; **134**:245–253.
24 Vermeulen K, Van Bockstaele DR, Berneman ZN. The cell cycle: a review of regulation, deregulation and therapeutic targets in cancer. *Cell Prolif* 2003; **36**:131–149.
25 Schwartz GK, Shah MA. Targeting the cell cycle: a new approach to cancer therapy. *J Clin Oncol* 2005; **23**:9408–9421.
26 Johansson M, Persson JL. Cancer therapy: targeting cell cycle regulators. *Anticancer Agents Med Chem* 2008; **8**:723–731.
27 Loewer A, Batchelor E, Gaglia G, Lahav G. Basal dynamics of p53 reveal transcriptionally attenuated pulses in cycling cells. *Cell* 2010; **142**:89–100.
28 Abbas T, Dutta A. p21 in cancer: intricate networks and multiple activities. *Nat Rev Cancer* 2009; **9**:400–414.
29 Blank M, Shiloh Y. Programs for cell death: apoptosis is only one way to go. *Cell Cycle* 2007; **6**:686–695.
30 Liu W, Huang XF, Qi Q, Dai QS, Yang L, Nie FF, *et al.* Asparanin A induces G(2)/M cell cycle arrest and apoptosis in human hepatocellular carcinoma HepG2 cells. *Biochem Biophys Res Commun* 2009; **381**:700–705.
31 Speidel D. Transcription-independent p53 apoptosis: an alternative route to death. *Trends Cell Biol* 2010; **20**:14–24.